Hindawi
Mathematical Problems in Engineering
Volume 2019, Article ID 2587373, 14 pages
https://doi.org/10.1155/2019/2587373

Research Article

Efficient Hybrid Method of FEA-Based RSM and PSO Algorithm for Multi-Objective Optimization Design for a Compliant Rotary Joint for Upper Limb Assistive Device

Ngoc Le Chau,[1] Hieu Giang Le,[1] Thanh-Phong Dao ,[2,3] Minh Phung Dang,[1] and Van Anh Dang[4]

[1] *Faculty of Mechanical Engineering, Ho Chi Minh City University of Technology and Education, Ho Chi Minh City, Vietnam*
[2] *Division of Computational Mechatronics, Institute for Computational Science, Ton Duc Thang University, Ho Chi Minh City, Vietnam*
[3] *Faculty of Electrical and Electronics Engineering, Ton Duc Thang University, Ho Chi Minh City, Vietnam*
[4] *Faculty of Mechanical Engineering, Industrial University of Ho Chi Minh City, Ho Chi Minh City, Vietnam*

Correspondence should be addressed to Thanh-Phong Dao; daothanhphong@tdtu.edu.vn

Received 18 December 2018; Revised 3 February 2019; Accepted 3 March 2019; Published 18 March 2019

Academic Editor: Alberto Borboni

This paper proposes an efficient hybrid methodology for multi-objective optimization design of a compliant rotary joint (CRJ). A combination of the Taguchi method (TM), finite element analysis (FEA), the response surface method (RSM), and particle swarm optimization (PSO) algorithm is developed to solving the optimization problem. Firstly, the TM is applied to determine the number of numerical experiments. And then, 3D models of the CRJ is built for FEA simulation, and mathematical models are formed using the RSM. Subsequently, the suitability of the regression equation is assessed. At the same time, the calculation of weight factors is identified based on the series of statistical equations. Based on the well-established equations, a minimum mass and a maximum rotational angle are simultaneously optimized through the PSO algorithm. Analysis of variance is used to analyze the contribution of design variables. The behavior of the proposed method is compared to the adaptive elitist differential evolution and cuckoo search algorithm through the Wilcoxon signed rank test and Friedman test. The results determined the weight factors of the mass and rotational angle are about 0.4983 and 0.5017, respectively. The results found that the optimum the mass and rotational angle are 0.0368 grams and 59.1928 degrees, respectively. It revealed that the maximum stress of 335 MPa can guarantee a long working time. The results showed that the proposed hybrid method outperforms compared to other evolutionary algorithms. The predicted results are close to the validation results. The proposed method is useful for related engineering fields.

1. Introduction

The stroke is one of the main causes resulting in either death or limited movement for many people in the word [1–4]. Limited movements of muscles affect their families and sociality. Although there are a lot of recent innovations, such as assistive devices, robotic rehabilitation systems, or exoskeletons to assist the upper limbs of disabled people [5–7], these devices had a large size and are of heavyweight [8]. Some researchers in the literature review focused on a design process and others investigated static and dynamic behaviors of the assistive devices [9]. It is known that the behaviors of the system can be effectively improved by good structural design or an optimal design process.

In order to enhance the quality of a product, an optimization process is a very necessary procedure. Nowadays, multiobjective optimization has been widely used to solve technical problems. For example, M. Costas et al. [10] used surrogate-based multi-objective optimization techniques to a crashworthiness problem in which the impact performance of a frontal crash absorber made of steel and a glass-fiber reinforced polyamide is optimized. J. Fang et al. [11] employed metamodel based multi-response objective-oriented sequential optimization to optimize the design of steel–aluminum hybrid structures for the highly nonlinear impact scenario

of rail. Y. Zhang et al. [12] used a hybrid optimal algorithm based on Monte Carlo simulation technique, Genetic algorithm, and Grey relational analysis to optimize tapered sandwich column for crashworthiness. Y. Zhang et al. [13] optimize a novel hierarchical circular tube using multi-objective optimization based on radial basis function, neural networks, and multi-objective particle swarm optimization algorithm. G. Sun et al. [14] used a heuristic optimization method to determine the value of the wall thickness of tailor rolled blank parts to maximize the energy absorption capacity. G. Zhou et al. [15] applied an enhanced hybrid and adaptive meta-model based global optimization to improve the performance of the steering system. G. Zhou et al. [16] proposed a multi-objective optimal algorithm using Latin hypercube sampling technique, orthogonal design, response surface model, radial-based importance sampling technique, and multi-objective particle swarm optimization algorithm to develop novel side door negative Poisson's ratio impact beam. G. Sun et al. [17] developed a multi-objective and multi-case reliability-based design optimization based on the radial basis function, the non-dominated sorting genetic algorithm II, and Monte Carlo simulation to optimize the tailor rolled blank hat-shaped structure. G. Sun et al. [18] used an iterative optimization algorithm with arrays to maximize the mass and minimize energy absorption capacity of hybrid structures for transverse loading. However, in the literature review, a multi-objective optimization problem for assistive devices has not received great interest yet. Therefore, the contribution of this study is to enter into a new entry related to a multiple response optimization for a rotary joint of upper limb assistive device.

In our design, a compliant rotary joint (CRJ) can support the forearm of disabled people in terms of handling their activities without a large dependence on their staffs and family members. It is known that the characteristics of an assistive device are influenced by the qualities of the proposed joint. Therefore, the present study proposes a multi-objective optimization of the CRJ. The CRJ is constructed based on a compliant mechanism (CM) that is an outperformed mechanism compared to conventional mechanisms due to its advantages, such as miniature size, being lightweight, increased accuracy, energy storage capability, and decreased vibrations [19–22]. The qualities of CRJ include a large rotational motion to be suitable for different people, being lightweight to be easily integrated into the upper limb, and minimal stress. The stress should be less than the allowed stress so as to guarantee long working fatigue without plastic failures.

Prior to implementing an optimization process for the CRJ, mathematical equations describing relations between the design parameters and the responses are actually desired. Although the mathematical models can be found by applying the theory of mechanics, they are difficult to achieve a precise equation. It is known that the CRJ is also a type of CMs, while the approximately mechanic theories for CMs are still large errors. In order to overcome such disadvantages and to achieve the above properties simultaneously for the CRJ, a new efficient approach of the Taguchi method (TM), finite element analysis (FEA), response surface method (RSM), and particle swarm optimization (PSO) algorithm is developed in this study. It can be considered as a surrogate-based soft computing optimization. It begins a collection of numerical data and then establishes the equation prior to implementing the optimization process. Commonly, a full factorial design can create the experimental matrix, but it requires a large number of experiments. Therefore, the TM is alternated with a sufficient number of experiments [22–25]. Although the TM reduces the number of experiments, it only optimizes a single quality response, while this study needs to solve the multi-objective responses, simultaneously. To implement a multi-objective optimization process, mathematical models must be established before starting the optimal process. Nowadays, many surrogate models have been used to represent the relationship between input variables and output responses such as RSM model [26, 27], Krigring model [28, 29], support vector regression [30], radial basis function [31], and adaptive neuro-fuzzy inference system [32]. Among them, RSM is an easy-to-use approximation model and able to accurately modeling [33]. Currently, RSM is still useful and valid for mathematical modeling in the field of engineering and industry [34, 35]. As a result, the RSM is integrating with the FEA to build the mathematical models in the present study. Then the PSO algorithm [36–39] is utilized. PSO is a multi-objective optimization technique that gives high precision results and fast convergence capabilities for linear and weak non-linear models. In the case of a strong non-linear model, the PSO algorithm needs to be modified or improved. For example, X. Hu and R.Eberhart [40] gave two ways to modify PSO: (i) In the initial population initialization process, all particles are repeated continuously until they meet all the constraints, and, (ii) during the calculation of the *pBest* and *gBest* values, only the locations in the feasible space are counted. N. B.Guedria [41] has improved PSO to overcome premature convergence and weak diversity when optimizing strong non-linear models. As mentioned, the CRJ must fulfill two objectives, including being lightweight and a large rotation angle. These two responses are contradictory. To optimize the multiple responses, most previous studies assigned the weight factor (WF) for each objective function according to the expert's experience or customer's requirements but a wrong experience may result in an unprecise optimal solution. Therefore, we follow a calculation of WF in [42].

The new contribution of this study is to develop an efficient hybrid integration for multi-objective optimization design of the CRJ. The hybrid method is a combination of the TM, FEA-based RSM, and PSO algorithm. In this study, a series of statistical equations are established to compute the WF for objective functions. Analysis of variance is utilized to investigate the significance of each design parameter. In addition, two statistical comparisons, Wilcoxon signed rank test, and Friedman test, are implemented to compare the behavior of the proposed hybrid method with other evolutionary algorithms. The prototype is built and evaluated to validate the optimal results.

2. Design for Compliant Torsion Spring

Figure 1 illustrates an assembled system of an upper limb rehabilitation device. It includes main parts: a CRJ (1) which

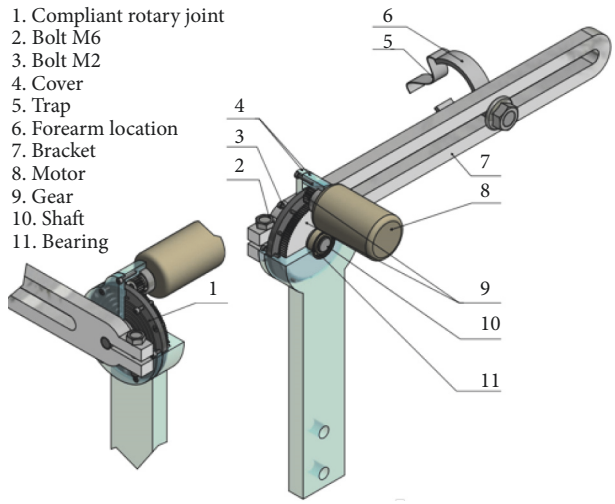

Figure 1: Model of the upper limb assistive device.

its outer ring is fixed to the cover (4) via three bolts (3). The inner diameter of the CRJ is fitted to the shaft (10) in which it is coupled with the passive gear (9). A Bracket (7) is connected to the shaft while the bracket is fitted to trap (5) which used to locate the forearm. The trap can be adjusted to be suitable for people's different arm sizes accordingly. The cover is mounted on the chair where a patient is seating. To perform the workout, the motor provides rotational motion for the bracket through the gear train. At this point, the CRJ is deformed a rotational angle. This deformation reduces the system's shock and ensures for the patient.

In the device, the CRJ is the most important part to guarantee a good rehabilitation process. The proposed CRJ needs to create a sufficiently large rotation angle larger than 50 degrees and small mass to fulfill being lightweight. However, it must also allow small stress to ensure the reliability for the rehabilitation process, as seen in Figure 2. Through many analyses and FEA simulations, it is discovered that the thickness (t) and diameter (D) mainly affect the outputs, such as the rotational angle, mass, and stress of the CRJ.

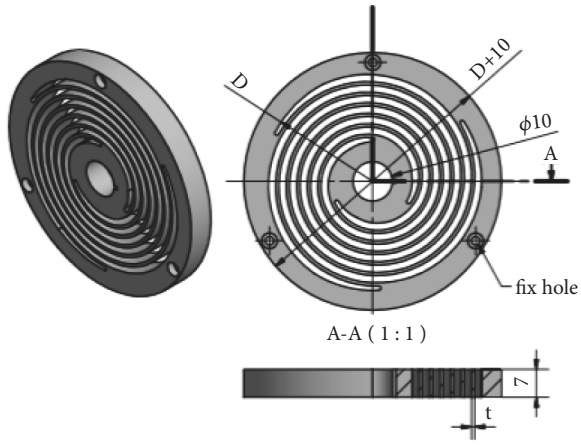

Figure 2: 2D and 3D model of compliant rotary joint.

3. Proposed Hybrid Methodology

3.1. Statement of Optimization Problem. According to the above design, a small mass is the first objective to permit being lightweight and a large rotational angle is the second objective so as to allow a wide application. Both objective functions are always conflicted but they are also simultaneously desired qualities for the CRJ in the rehabilitation device. Besides, resulting stress should be also under the yield strength of the proposed material so that the CRJ can operate without plastic failures. Because the CRJ is constructed based on the concept of CMs [19–22], a field of non-traditional mechanical engineering, the quality characteristics of joint greatly depend on the thickness and length of the leaf springs. If the twisted step of leaf springs is constant, the length of leaf spring depends on the diameter of the CRJ. Hence, the thickness t and diameter D are two design parameters, while the mass and rotational angle are two output responses. Furthermore, the stress is a necessary constraint for the joint.

As aforementioned, if the performances of CRJ are improved, the efficiency of the assistive device for an upper limb is enhanced accordingly. The multiple-objective optimization problem is briefly stated as follows:

Determine the design variables: D and t.

Minimize the mass:

$$f_1(D,t). \tag{1}$$

Maximize the rotational angle:

$$50^o \le f_2(D,t) \le 60^o. \tag{2}$$

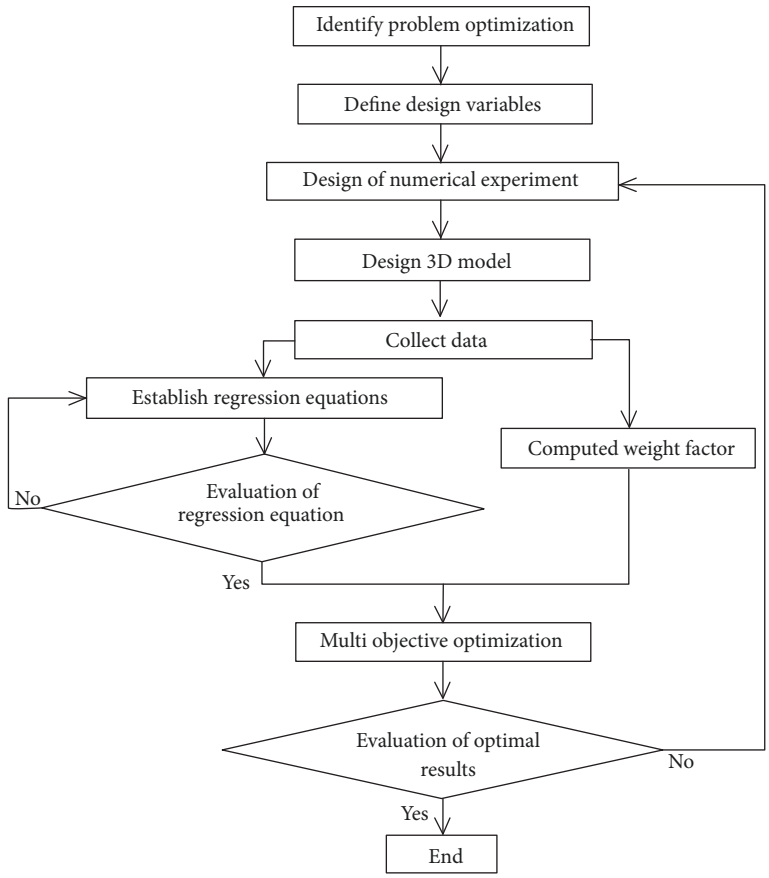

Figure 3: Flowchart for multiple objective optimization process for the CRJ.

Subject to constraints:

$$52 \text{ mm} \leq D \leq 56 \text{ mm} \tag{3}$$

$$0.8 \text{ mm} \leq t \leq 1.2 \text{ mm}, \tag{4}$$

$$f_3(D,t) \leq 335 \text{ MPa}, \tag{5}$$

where f_1 is the mass, f_2 is the rotational angle, and f_3 is the stress.

3.2. Methodology. In order to conduct the multiple objective optimization problems for the CRJ, a surrogate-based optimization method is implemented. It starts with the establishment of the number of numerical data through the TM. And then, the FEA is used to collect the numerical data. Two mathematical models for both responses are built based on the RSM. Finally, the PSO algorithm is utilized to optimize simultaneously both quality responses. A hybrid optimization algorithm is an integration of the TM, FEA-based RSM, and PSO. Figure 3 depicts the flowchart of the optimal process of CRJ. It consists of main steps as follows.

Step 1 (identifying optimization problem). Basically, the CRJ has to be lightweight and requires a large moving range and an ensured durability.

Step 2 (definingdesign variables). The required characteristics of the CRJ depend on two key parameters, including the thickness of leaf spring and diameter of CRJ. Two chosen design variables for optimization are diameter D and thickness t. The relationship between the design parameters and output responses can be presented by the following formula:

$$y = f(x_1, x_2, \ldots x_n) + \varepsilon \tag{6}$$

where y is the function of output, $x_1, x_2, \ldots, x_n$ denote the independent variables, n is the number of independent variables, and ε is an error.

Step 3 (designing 3D model and collecting data). The TM is utilized to set up the number of numerical experiments. Then, 3D models are drawn and the FEA is used to retrieve the quality characteristics.

Step 4 (calculating weight factor). It is well-known that the mass is desired as small as possible while the rotational angle is needed as large as possible. Therefore, the designer must balance among them. In fact, almost designers use their experience to choose the WF for each objective function. However, this choice is random, so the optimal results may result in an unprecise solution. In order to determine the correct WF, there are many ways to calculate WF. For

instance, WF is calculated by combining the grey relational analysis with the entropy measurement technique [43]. The grey relational analysis is coupled with principal component analysis [25]. The total score of each pepper was used to calculate the weight [44]. Unlike previous studies, the present study is based on the sensitivity of responses, an effect of design variables on the responses, and statistical-based equation sets were established to produce weighting formulas. This study follows a statistical method based on signal-to-noise (*S/N)* ratio [42]. One of the most important tasks is that each objective function should be normalized in the range $[0, 1]$. The TM with the *S/N* ratio shows a better quality response corresponding to a larger *S/N* ratio value. In this work, two objective functions are expected as follows.

The smaller-the-better is used for the mass by following equation:

$$\eta = -10 \log \left(\frac{1}{n} \sum_{1}^{n} f_i^2 \right). \tag{7}$$

The larger-the-better is utilized for the rotational angle as follows:

$$\eta = -10 \log \left(\frac{1}{n} \sum_{1}^{n} \frac{1}{f_i^2} \right). \tag{8}$$

where f is the value of the response and n the number of replicates of experiment i_{th}.

Normalized *S/N* of each objective function was implemented by the following formula:

$$z_i = \frac{\eta_i - \min \eta_i}{\max \eta_i - \min \eta_i}, \tag{9}$$

where z_i is the normalized mean *S/N* value for the i_{th} response ($i = 1, 2, \ldots, n$), n is the number of responses, and η_i illustrates the estimated *S/N* value from the TM. $\max\eta_i$ and $\min\eta_i$ are the largest and smallest values of η_i, respectively.

The average value of normalized *S/N* ratios for each objective function was calculated by the following formula:

$$a_{Li} = \frac{1}{m_{Lij}} \sum_{i=1}^{m} z_{\mathrm{ij}}, \tag{10}$$

where a_{Li} is the average value of *S/N* ratio of level i_{th} of each design variable of each objective function. m_{Lji} is a number of repetitions of level i_{th}. z_{ij} is the value of *S/N* ratio of level i_{th} of objective function j_{th}.

The rank of each level of each design variable was determined as follows:

$$\begin{aligned} r_{ij} = {} & \max \left\{ z_{i,j,1}, z_{i,j,2}, \ldots, z_{i,j,r} \right\} \\ & - \min \left\{ z_{i,j,1}, z_{i,j,2}, \ldots, z_{i,j,r} \right\}, \end{aligned} \tag{11}$$

where r_{ij} is the mean rank (max-min) of the normalized mean *S/N* ratio for each level of each design parameter $j = 1, 2, ..q$, q is the number of design parameters, $r = 1, 2, ..l$, l is the number of experimental level of each objective. $z_{i,j,r}$ is the normalized mean value of *S/N* for the i_{th} response of the parameter j_{th} at the k_{th} experiment.

Table 1: Design variables and their levels.

Parameters	Level 1	Level 2	Level 3
D (mm)	52	54	56
t (mm)	0.8	1.0	1.2

The WF of each objective function was calculated as follows:

$$w_i = \frac{\sum_{j=1}^{q} r_{ij}}{\sum_{i=1}^{n} \sum_{j=1}^{q} r_{ij}}, \tag{12}$$

where w_i is the weight factor of objective i_{th}

Step 5 (establishing regression equation). The RSM is then used to establish the regression equations to describe a relationship between the design variables and quality responses. Because these relations are almost nonlinear, a full quadratic form was a suitable model for the CRJ as follows [45]:

$$f_k = \beta_0 + \sum_{i=1}^{n} \beta_i x_i + \sum_{i=1}^{n} \beta_{ii} x_i^2 + \sum_{i=1}^{n-1} \sum_{j=i+1}^{n} \beta_{ij} x_i x_j + \varepsilon_i, \tag{13}$$

where β_i are unknown regression coefficients; β_{ii} are quadratic coefficients; β_{ij} are interaction coefficients, x_1, x_2,...x_n are a set of n predictor believed to be related to a response variable f_k, ε_i random error.

The analysis of variance (ANOVA) also performs evaluating the contribution of the parameter.

Step 6 (validating the precision of regression equation). The established regression equation often has an undesired error. Hence, to evaluate the prediction precision of those equations, some random values of the design variables are chosen to build 3D models. And then, the FEA simulations are compared with the predicted results from the regression equation. If the error is large, several types of regression equations are recalculated to form new mathematical equations.

Step 7 (optimization). The regression equations were determined in Step 5 and validated in Step 6. At the same time, the WFs are computed in Step 4. At last, the optimization process is implemented by programming the multi-objective PSO algorithm in MATLAB.

4. Results and Discussion

4.1. Numerical Data and Regression Equations. Firstly, the TM was utilized to refine the design parameters to achieve a good initialization for the CRJ. The two design variables of CRJ, including the diameter D and the thickness t, were divided into three levels, as given in Table 1. A matrix of numerical experiments was established by using the L_9 orthogonal array. And then, nine models of CRJ were drawn by Inventor software. Numerical experiments were

Table 2: Results of numerical experiments.

No.	D (mm)	t (mm)	Mass, f_1 (Gram)	Angle, f_2 (degree)	Stress, f_3 (Mpa)
1	52	0.8	0.0328	56.55	398.00
2	52	1	0.0355	37.42	251.57
3	52	1.2	0.0381	23.57	172.08
4	54	0.8	0.0345	59.79	379.28
5	54	1	0.0373	40.99	248.74
6	54	1.2	0.0402	26.37	177.14
7	56	0.8	0.0361	62.51	362.21
8	56	1	0.0392	44.28	247.33
9	56	1.2	0.0423	29.16	185.38

Table 3: ANOVA for the mass.

No.	Source	Degrees of freedom (DoF)	Contribution (%)	F-Value	P-Value
1	D	1	29.46	2914851.94	0.001
2	t	1	70.20	6946032.12	0.001
3	D^2	1	0.00	70.14	0.004
4	t^2	1	0.00	0.03	0.871
5	$D * t$	1	0.34	34001.67	0.001
6	Error	3	0.00		
7	Total	8	100.00		

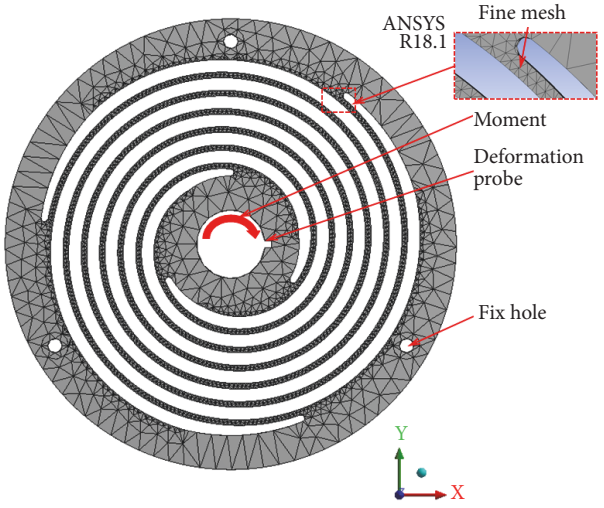

Figure 4: Meshing model and boundary conditions.

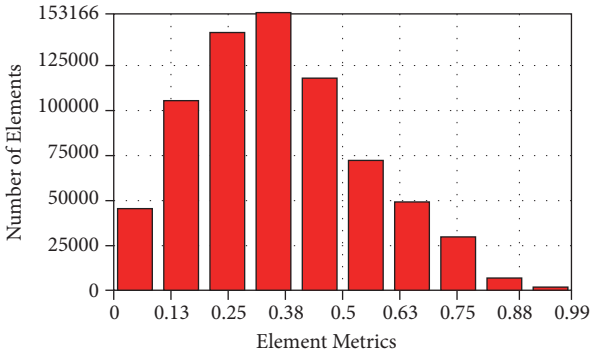

Figure 5: Evaluating the quality of the meshing.

performed to collect data by FEA in ANSYS. The mesh model and boundary conditions were set up, as seen in Figure 4. The CRJ model was fixed by three holes, a moment applied to the inner hole. Al7075 was chosen as the material for the CRJ because of its light density of 2770 kg/m^3, a high yield strength of 503 MPa, Young modulus of 72000 MPa, and Poisson's ratio of 0.33. The face sizing method was chosen for meshing. The main parameters of the meshed model included the element size of 0.3 mm, the number nodes of 1243588, and the number of elements of 720074. Based on the Skewness criteria, the results indicated that the element metrics are within the range value from 0.25 to 0.5. as seen in Figure 5. According to the Skewness in ANSYS, this range proved that the accuracy of finite element models is relatively good [46]. The results of the analysis are presented in Table 2.

Based on the data from Table 2, the RSM was used to determine the mathematical equations for the mass. The results found the determination coefficient (R^2) of the equation is almost 100%. It can be concluded that the regression equation is a good predictor for the mass. According to statistical theory, the p-value of a design parameter is larger than 0.05 that parameter is not statistically significant. However, the parameters still had a certain influence on the mass, and

Table 4: ANOVA for the rotational angle.

No.	Source	DoF	Contribution (%)	F-Value	P-Value
1	D	1	3.27	412.15	0.001
2	t	1	96.19	12118.95	0.001
3	D^2	1	0.00	0.26	0.645
4	t^2	1	0.51	64.24	0.004
5	$D * t$	1	0.00	0.26	0.644
6	Error	3	0.02		
7	Total	8	100.00		

Table 5: ANOVA for the stress.

No.	Source	(DoF)	Contribution	F-Value	P-Value
1	D	1	0.19%	21.44	0.019
2	t	1	96.04%	10979.99	0.001
3	D^2	1	0.00%	0.39	0.576
4	t^2	1	2.80%	319.82	0.001
5	$D * t$	1	0.95%	108.47	0.002
6	Error	3	0.03%		
7	Total	8	100.00%		

all parameters were included in the regression equation. The regression equation for the mass was achieved as follows:

$$f_1 = 0.01746 - 0.000112D - 0.018911t - 0.000004D^2 + 0.000008t^2 + 0.000616Dt \quad (14)$$

ANOVA was then used to determine the significant contribution or sensitivity analysis of each factor on the mass. As seen in Table 3, the results revealed the contribution level of D approximately 29.46%, of t approximately 70.20%, and of $D * t$ approximately 0.34%. As a result, to reduce the mass of the CRJ, the value of the thickness t should be reduced, since the contribution of t is greater than D.

In a similar procedure, the mathematical model for rotational angle was built via the RSM. The results find out that R^2 is approximately 99.98%. It showed the established regression equation for the rotational angle is relatively well. The regression equation for the rotation angle was established as follows:

$$f_2 = -16 + 5.38D - 175.2t - 0.0334D^2 + 52.41t^2 - 0.236Dt. \quad (15)$$

Then, the contribution of each design variable on the rotational angle was identified using ANOVA. Table 4 shows that the contribution levels of D, t, t^2 are approximately 3.27%, 96.19%, and 0.51%, respectively. It can conclude that the influence of t to the rotation angle is highest. To increase the rotational angle, it is necessary to decrease the thickness t.

Finally, the RSM was also applied to establish the regression equation for the stress. The results given the R^2 is approximately 99.97%. It is noted that the regression equation

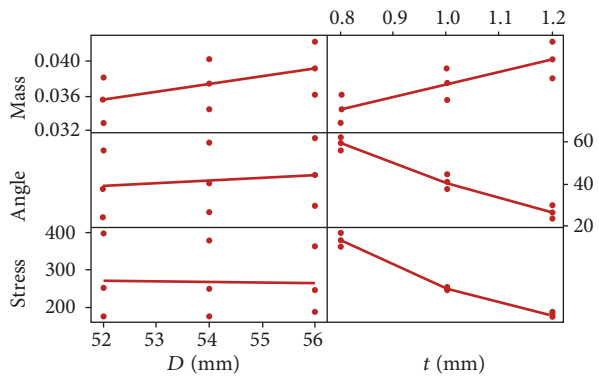

Figure 6: Sensitivity analysis of design variables.

is relatively accurate. The equation for the stress was given as follows:

$$f_3 = 4034 - 61D - 3651t - 0.26D^2 + 745t^2 + 30.68Dt. \quad (16)$$

ANOVA was analyzed for the stress. The results of Table 5 give that the contribution levels of D, t, D^2, t^2, $D * t$ are 0.19%, 96.04%, 0.00%, 2.80%, and 0.95%, respectively. It shows that the contribution of t to the stress is largest. The contribution level of D was not significant. To reduce stress, the thickness t should be increased.

The statistical-based sensitivity analysis was used to confirm how different values of the variables on each output response. As seen in Figure 6, factor D has a value from 52 mm to 56 mm; this parameter affected the mass and the angle in increase slightly, the stress in decrease slightly. Factor t has a value from 0.8 mm to 1.2 mm, the mass in increase slightly.

Table 6: Evaluating the precision of mathematical models.

Parameter	predicted			FEA			Error (%)		
	Mass (gram)	Stress (MPa)	Angle (degree)	Mass (gram)	Stress (MPa)	Angle (degree)	Mass	Stress	Angle
D = 53 mm; t = 8.8 mm	0.0337	388.17	58.69	0.0337	387.77	58.22	0.28	0.1	0.81
D = 54 mm t = 0.9 mm	0.036	306.76	50.43	0.0359	312.94	50.15	0.3	2.02	0.55
D = 55 mm t = 1.2 mm	0.0414	181.98	28.52	0.0413	187.17	27.79	0.27	2.85	2.57
Average							0.28	1.66	1.33

Table 7: *S/N* ratio values and normalized *S/N* values.

No.	*D (mm)*	*t (mm)*	*S/N* ratio of f_1 (dB)	*S/N* ratio of f_2 (dB)	Normalized *S/N* of f_1	Normalized *S/N* of f_2
1	52	0.8	-29.68	35.0487	0	0.897266
2	52	1.0	-29.00	31.4621	0.310995	0.473912
3	52	1.2	-28.38	27.4472	0.588876	0
4	54	0.8	-29.24	35.5326	0.19866	0.954388
5	54	1.0	-28.57	32.2536	0.505447	0.567337
6	54	1.2	-27.92	28.4222	0.79981	0.115089
7	56	0.8	-28.85	35.919	0.376887	1
8	56	1.0	-28.13	32.9242	0.700775	0.646493
9	56	1.2	-27.47	29.2958	1	0.218201

Table 8: Results of weight factor.

Parameter	Mean of *S/N* ratio f_1			Mean of *S/N* ratio f_2			Rank	
	level 1	level 2	level 3	level 1	level 2	Level 3	f_1	f_2
D	0.3000	0.5013	0.6926	0.4571	0.5456	0.6216	0.3926	0.1645
t	0.1918	0.5057	0.7962	0.9506	0.5626	0.1111	0.6044	0.8395
Weight factor							0.4983	0.5017

The factor t affected stress in the 0.8 mm to 1 mm range, decreasing rapidly from 1.0 mm to 1.2 mm range and affected to the angle in decrease slightly.

4.2. Precision of the Regression Equation. After the regression equations were established. As mentioned in the previous section, although the value R^2 of three equations was relatively good, it still needs a step so as to determine the prediction precision of these equations. Three models of CRJ were drawn based on randomly selected parameters. Subsequently, these models were simulated through FEA in ANSYS 2018 software. As seen in Table 6, the average error of the mass is of 0.28%, the stress of 1.66%, and the angle of 1.33%. These errors are very small, and so the mathematical models are reliable for prediction.

4.3. Computation of Weight Factor. The numerical data of the mass and the rotational angle were converted to *S/N* ratios by (7)-(8), respectively. And then, the *S/N* ratios were normalized to eliminate the effect of the unit factor using (9), as given in Table 7. The average value of normalized *S/N* ratios for each objective function was computed by using (10). The rank of each level of each design variable was determined by (11). The weight factor was calculated by (12), as given in Table 8. The weights of f_1 and f_2 were 0.4983 and 0.5017 respectively.

Table 9: Optimal results.

D (mm)	t (mm)	f_1 (gram)	f_2 (degree)	f_3 (MPa)
56	0.841	0.0368	59.1928	335

4.4. Optimal Results. The optimal results were achieved by the PSO algorithm in MATLAB R2014a. The main parameters for PSO algorithm, such as the population size of 25 and tolerance of 10-6 and maximum iteration of 5000, were set. The optimal results were found out the dimension D of 56 mm and t of 0.841 mm. The optimum value of the mass, the rotation angle, and the stress are 0.0368 grams and 59.1928 degrees, respectively. The resulting stress was about 335 MPa that is still less than the yield strength of material. It permits a long working time for the CRJ, as given in Table 9.

4.5. Statistical Analysis. This section provided a statistical analysis so as to evaluate and compare the hybrid method

Table 10: Pareto-optimal solution.

No.	Pareto-optimal solution of AEDE		Pareto-optimal solution of PSO		Pareto-optimal solution of Cuckoo	
	f_1 (gram)	f_2 (degree)	f_1 (gram)	f_2 (degree)	f_1 (gram)	f_2 (degree)
1	0.03684694	59.1926	0.03684698	59.1928	0.03640000	56.4125
2	0.03684698	59.1927	0.03684698	59.1928	0.03680000	57.6736
3	0.03684699	59.1926	0.03684698	59.1928	0.03560000	54.7656
4	0.03684701	59.1926	0.03684698	59.1928	0.03650000	54.2459
5	0.03684701	59.1926	0.03684698	59.1928	0.03690000	54.6147
6	0.03684698	59.1926	0.03684698	59.1928	0.03640000	53.6284
7	0.03684698	59.1927	0.03684698	59.1928	0.03620000	55.6318
8	0.03684698	59.1927	0.03684698	59.1928	0.03730000	56.4305
9	0.03684697	59.1928	0.03684698	59.1928	0.03500000	49.8407
10	0.03684697	59.1927	0.03684698	59.1928	0.03540000	53.9830
11	0.03684698	59.1927	0.03684698	59.1928	0.03740000	52.1104
12	0.03684696	59.1927	0.03684698	59.1928	0.03650000	55.2316
13	0.03684698	59.1926	0.03684698	59.1928	0.03700000	54.0561
14	0.03684698	59.1927	0.03684698	59.1928	0.03550000	51.5698
15	0.03684697	59.1927	0.03684698	59.1928	0.03660000	57.9326
16	0.03684698	59.1927	0.03684698	59.1928	0.03720000	50.7281
17	0.03684699	59.1927	0.03684698	59.1928	0.03600000	56.0966
18	0.03684696	59.1927	0.03684698	59.1928	0.03580000	53.2667
19	0.03684699	59.1927	0.03684698	59.1928	0.03720000	56.3933
20	0.03684699	59.1926	0.03684698	59.1928	0.03610000	55.3665
21	0.03684698	59.1927	0.03684698	59.1928	0.03760000	54.3757
22	0.03684697	59.1927	0.03684698	59.1928	0.03460000	49.3076
23	0.03684698	59.1927	0.03684698	59.1928	0.03500000	51.9317
24	0.03684698	59.1928	0.03684698	59.1928	0.03580000	50.4642
25	0.03684697	59.1927	0.03684698	59.1928	0.03640000	52.0670
26	0.03684699	59.1927	0.03684698	59.1928	0.03590000	55.9478
27	0.03684700	59.1926	0.03684698	59.1928	0.03560000	51.7925
28	0.03684697	59.1927	0.03684698	59.1928	0.03540000	49.4596
29	0.03684698	59.1927	0.03684698	59.1928	0.03430000	48.3116
30	0.03684697	59.1928	0.03684698	59.1928	0.03730000	47.2540

Table 11: Wilcoxon's comparison the proposed hybrid method with AEDE for the mass.

Number for tests	Median of difference	p-value	Wilcoxon statistic
30	0.000	0.821	244
	Null hypothesis: H_0: Median of difference are zero		
	Alternative hypothesis: H_1: Median of difference are not zero		

to other evolutionary algorithms, such as the adaptive elitist differential evolution [47] and cuckoo search algorithm [48–51]. The Wilcoxon's rank signed test and Friedman test [52–54] were both applied to evaluate the effectiveness of the proposed hybrid method. The numerical simulations were conducted 30 runs for each algorithm. The Pareto-optimal solution was achieved, as given in Table 10. Table 10 shows that ADED and CUCKOO algorithms have small differences in function values *f1* and *f2*, in which the PSO algorithm proven function *f1* and *f2* are the same. This means the convergence of ADED and CUCKOO algorithms is lower than the PSO algorithm, because each algorithm has given different Pareto. Therefore, Wilcoxon's comparison and Friedman Test are used to compare the behavior of algorithms. The Wilcoxon's rank signed test was performed at 5% significant level and 95% confidence intervals. The results of Wilcoxon's rank signed test were given in Tables 11–14.

Table 11 gives the result of statistical analysis for the mass by comparing the proposed hybrid method with the AEDE. It showed the P-value is greater than 0.05. This suggests that the null hypothesis (H_0) is accepted. It means that the predicted mass of the two algorithms was the same. However, the statistical analysis for the angle in Table 12 shows that the null hypothesis (H_0) is not accepted. It means that the predicted angles of the two algorithms are different. The predicted angle of the proposed hybrid method is higher than of the AEDE

Table 12: Wilcoxon's comparison the proposed hybrid method with AEDE for the angle.

Number for tests	Median of difference	p-value	Wilcoxon statistic
30	-0.0000799	0.001	7
	Null hypothesis: H_0: Median of difference are zero		
	Alternative hypothesis: H_1: Median of difference are not zero		

Table 13: Wilcoxon's comparison of the proposed hybrid method with cuckoo for the mass.

Number for tests	Median of difference	p-value	Wilcoxon statistic
30	0.000647	0.001	389
	Null hypothesis: H_0: Median of difference are zero		
	Alternative hypothesis: H_1: Median of difference are not zero		

Table 14: Wilcoxon's comparison of the proposed hybrid method with cuckoo for the angle.

Number for tests	Median of difference	p-value	Wilcoxon statistic
30	5.7454300	0.001	465
	Null hypothesis: H_0: Median of difference are zero		
	Alternative hypothesis: H_1: Median of difference are not zero		

Table 15: Friedman Test for the mass.

Response	Number of tests	Median of difference	Sum of Ranks
Mass by AEDE	30	0.036847	66
Mass by the proposed hybrid method	30	0.036847	68
Mass by cuckoo	30	0.036544	46
Overall	90	0.036746	
DF	Chi-Square	P-Value	
2	9.87	0.007	
Null hypothesis: H_0: All treatment effects are zero			
Alternative hypothesis H_1: Not all treatment effects are zero			

algorithm. Thus, the proposed hybrid method algorithm was more efficient than the AEDE algorithm, as given in Tables 11-12.

Similarly, statistical analysis for the mass and angle by comparing the proposed hybrid method with the cuckoo search algorithm. Table 13 showed that the null hypothesis (H_0) is not accepted. The optimal predicted mass from the proposed hybrid method is lower than that from the cuckoo search algorithm. Thus, the cuckoo algorithm is more efficient. However, when analyzing the statistics for the angle, the predicted angle result of the proposed hybrid method is greater than that of the cuckoo algorithm, as shown in Table 14. This means that the proposed hybrid method is more efficient than the cuckoo algorithm.

Another way, the Friedman Test, a non-parametric approach, is an alternative to the one-way ANOVA with repeated measures. This approach would determine the difference between the optimization algorithms at significant levels of $\alpha = 0.05$. The Friedman test for the mass and angle were conducted, separately. The numerical simulations were conducted 30 runs for each algorithm.

Table 15 shows the P-value was smaller than 0.05, so the null hypothesis was not accepted. The predicted mass from proposed hybrid method differed from the other optimal algorithms. The sum of ranks of cuckoo search algorithm was the smallest. So, the cuckoo algorithm was the most effective. Similarly, Table 16 gives that the predicted angles of the optimal algorithms were different, but the proposed hybrid method was the best.

In summary, the results of Wilcoxon's comparative and Friedman Test methods indicated that the proposed hybrid method was more effective than the AEDE and cuckoo search algorithm. Therefore, the proposed hybrid method was reliable to optimize the proposed CRJ.

5. Validations

Based on Wilcoxon's comparison and the Friedman Test, the Pareto-optimal solution of PSO is selected. Based on Table 10, the Pareto of the PSO algorithm is similar, and the value of mass and angle are 0.03684698 grams and 59.1928, respectively, when the value of the diameter is 56 mm and the thickness is 0.841 mm. Then a 3D prototype of CRJ was created. The stress distribution was given, as seen in Figure 7. The mass of 0.036 grams, the angle of 58.8067 degrees, and stress of 326.63 MPa. The results revealed that the errors of mass, stress, and rotational angle are 0.31%, 1.98%, and 2.08%, respectively, given in Table 17. These errors came from the size

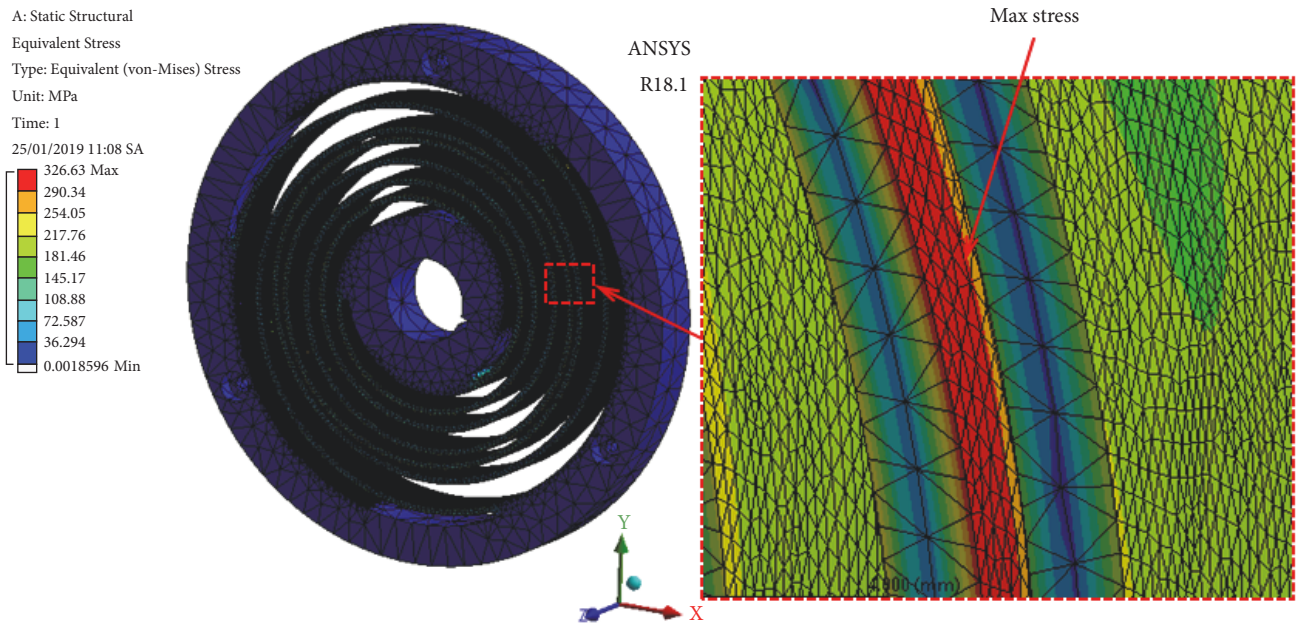

Figure 7: Stress distribution.

Table 16: Friedman Test for the angle.

Response	Number of tests	Median of difference	Sum of Ranks
Mass by AEDE	30	59.1927	62
Mass by the proposed hybrid method	30	59.1928	88
Mass by cuckoo	30	54.0196	30
Overall	90	57.4683	
DF	Chi-Square	P-Value	
2	56.27	0.001	
Null hypothesis: H_0: All treatment effects are zero			
Alternative hypothesis H_1: Not all treatment effects are zero			

Table 17: Comparison of predicted results and validation results.

Response	Predicted result	Validation results	Error (%)
f_1 (gram)	0.0368	0.0367	0.2725
f_2 (degree)	59.1928	58.8067	0.6567
f_3 (MPa)	335	326.63	2.5625

tolerances and modeling. For such a small error, the proposed hybrid method had good reliability that can be applied for optimizing the parameters for the assistive devices and related engineering.

6. Conclusions

In this paper, a new hybrid method was proposed for conducting the multi-objective optimization design so as to improve the performing efficiency of CRJ. The proposed integration was combined of the TM, FEA, the RSM, and the PSO algorithm.

Firstly, the TM was applied to make the number of numerical experiments. Subsequently, the FEA simulations were programmed so as to collect the data. Based on the data, the mathematical models for both the mass and rotational angle were built using the RSM, and the WF of each quality response was computed. The precision of regression equations was relatively good. Using the well-established equations, the optimization problem was solved through the PSO algorithm.

The WF of the mass of 0.4983 and the WF rotational angle of 0.5017 were determined. ANOVA results showed that the CRJ thickness has the most effect. The accuracy

of mathematical models was evaluated by the coefficient and randomized testing. Valuation results revealed that the coefficients of determination of mass, angle, and stress are 100%, 99.98%, and 99.97% respectively. The average error of the predicted models and FEA is about 0.28, 1.66, and 1.33 corresponding to the volume, angle, and stress.

The behavior of the proposed hybrid method was better than that of the adaptive elitist differential evolution and cuckoo search algorithm through using the Wilcoxon signed rank test and Friedman test.

The optimal result was found out for the dimension D of 56 mm and thickness t of 0.841 mm for the CRJ. The optimal mass of 0.036 g and optimal rotational angle of 59.1928 degrees were found with minimal stress of 335 MPa. The errors between the predicted and the validation results for the mass, stress, and rotation angle are 0.2725%, 0.6567%, and 2.5625%, respectively. The small error showed that the proposed optimization is reliable to solve for multiple optimization problems for the CRJ and related complex optimization problems.

Data Availability

The data used to support the findings of this study are included within the article.

Conflicts of Interest

The authors declare that there are no conflicts of interest regarding the publication of this article.

Acknowledgments

The authors are thankful for the financial support from the HCMC University of Technology and Education, Vietnam, under Grant no. T2019-02NCS.

References

[1] K. Kiguchi, M. H. Rahman, M. Sasaki, and K. Teramoto, "Development of a 3DOF mobile exoskeleton robot for human upper-limb motion assist," *Robotics and Autonomous Systems*, vol. 56, no. 8, pp. 678–691, 2008.

[2] J. M. Ibarra Zannatha, A. J. M. Tamayo, Á. D. G. Sánchez, J. E. L. Delgado, L. E. R. Cheu, and W. A. S. Arévalo, "Development of a system based on 3D vision, interactive virtual environments, ergonometric signals and a humanoid for stroke rehabilitation," *Computer Methods and Programs in Biomedicine*, vol. 112, no. 2, pp. 239–249, 2013.

[3] H. S. Lo and S. Q. Xie, "Exoskeleton robots for upper-limb rehabilitation: state of the art and future prospects," *Medical Engineering & Physics*, vol. 34, no. 3, pp. 261–268, 2012.

[4] N. Le Chau, S.-C. Huang, T.-P. Dao, and H. G. Le, "Design and analysis of a new gear-driven compliant torsional spring for upper-limb biomedical rehabilitation device," in *Proceedings of the 2017 IEEE International Conference on Systems, Man, and Cybernetics, SMC 2017*, pp. 40–45, Canada, October 2017.

[5] K. P. Michmizos and H. I. Krebs, "Pediatric robotic rehabilitation: current knowledge and future trends in treating children with sensorimotor impairments," *NeuroRehabilitation*, vol. 41, no. 1, pp. 69–76, 2017.

[6] S. Masiero, P. Poli, G. Rosati et al., "The value of robotic systems in stroke rehabilitation," *Expert Review of Medical Devices*, vol. 11, no. 2, pp. 187–198, 2014.

[7] J. Borg, A. Lindström, and S. Larsson, "Assistive technology in developing countries: a review from the perspective of the convention on the rights of persons with disabilities," *Prosthetics and Orthotics International*, vol. 35, no. 1, pp. 20–29, 2011.

[8] Z.-W. Yang and C.-C. Lan, "An adjustable gravity-balancing mechanism using planar extension and compression springs," *Mechanism and Machine Theory*, vol. 92, pp. 314–329, 2015.

[9] N. Paine, J. S. Mehling, J. Holley et al., "Actuator control for the NASA-JSC valkyrie humanoid robot: a decoupled dynamics approach for torque control of series elastic robots," *Journal of Field Robotics*, vol. 32, no. 3, pp. 378–396, 2015.

[10] M. Costas, J. Díaz, L. Romera, and S. Hernández, "A multi-objective surrogate-based optimization of the crashworthiness of a hybrid impact absorber," *International Journal of Mechanical Sciences*, vol. 88, pp. 46–54, 2014.

[11] J. Fang, N. Qiu, X. An, F. Xiong, G. Sun, and Q. Li, "Crashworthiness design of a steel–aluminum hybrid rail using multi-response objective-oriented sequential optimization," *Advances in Engineering Software*, vol. 112, pp. 192–199, 2017.

[12] Y. Zhang, X. Xu, G. Sun, X. Lai, and Q. Li, "Nondeterministic optimization of tapered sandwich column for crashworthiness," *Thin-Walled Structures*, vol. 122, pp. 193–207, 2018.

[13] Y. Zhang, X. Xu, J. Wang, T. Chen, and C. H. Wang, "Crushing analysis for novel bio-inspired hierarchical circular structures subjected to axial load," *International Journal of Mechanical Sciences*, vol. 140, pp. 407–431, 2018.

[14] G. Sun, J. Tian, T. Liu, X. Yan, and X. Huang, "Crashworthiness optimization of automotive parts with tailor rolled blank," *Engineering Structures*, vol. 169, pp. 201–215, 2018.

[15] G. Zhou, W. Zhao, L. Duan, C. Wang, and G. Chen, "Optimisation design of a steering system based on E-HAM algorithm," *International Journal of Vehicle Design*, vol. 75, no. 1-4, pp. 124–138, 2017.

[16] G. Zhou, W. Zhao, Z.-D. Ma, C. Wang, and Y. Wang, "Multi-objective reliability design optimization of a novel side door negative Poisson's ratio impact beam," *Proceedings of the Institution of Mechanical Engineers, Part D: Journal of Automobile Engineering*, vol. 232, no. 9, pp. 1196–1205, 2018.

[17] G. Sun, H. Zhang, J. Fang, G. Li, and Q. Li, "Multi-objective and multi-case reliability-based design optimization for tailor rolled blank (TRB) structures," *Structural and Multidisciplinary Optimization*, vol. 55, no. 5, pp. 1899–1916, 2017.

[18] G. Sun, H. Yu, Z. Wang, Z. Xiao, and Q. Li, "Energy absorption mechanics and design optimization of CFRP/aluminium hybrid structures for transverse loading," *International Journal of Mechanical Sciences*, vol. 150, pp. 767–783, 2019.

[19] T.-P. Dao, S.-C. Huang, and N. Le Chau, "Robust parameter design for a compliant microgripper based on hybrid Taguchi-differential evolution algorithm," *Microsystem Technologies*, vol. 24, no. 3, pp. 1461–1477, 2018.

[20] N. L. Ho, T. Dao, H. G. Le, and N. L. Chau, "Optimal design of a compliant microgripper for assemble system of cell phone vibration motor using a hybrid approach of ANFIS and Jaya," *Arabian Journal for Science and Engineering*, vol. 44, no. 2, pp. 1205–1220, 2018.

[21] N. L. Chau, T.-P. Dao, and V. T. T. Nguyen, "Optimal design of a dragonfly-inspired compliant joint for camera positioning system of nanoindentation tester based on a hybrid integration

of Jaya-ANFIS," *Mathematical Problems in Engineering*, vol. 2018, Article ID 8546095, 16 pages, 2018.

[22] T.-P. Dao, N. L. Ho, T. T. Nguyen et al., "Analysis and optimization of a micro-displacement sensor for compliant microgripper," *Microsystem Technologies*, vol. 23, no. 12, pp. 5375–5395, 2017.

[23] S. Dharmalingam, R. Subramanian, K. Somasundara Vinoth, and B. Anandavel, "Optimization of tribological properties in aluminum hybrid metal matrix composites using gray-taguchi method," *Journal of Materials Engineering and Performance*, vol. 20, no. 8, pp. 1457–1466, 2011.

[24] M. Zhou, L. Kong, L. Xie, T. Fu, G. Jiang, and Q. Feng, "Design and optimization of non-circular mortar nozzles using finite volume method and Taguchi method," *The International Journal of Advanced Manufacturing Technology*, vol. 90, no. 9-12, pp. 3543–3553, 2017.

[25] G. Sun, H. Zhang, J. Fang, G. Li, and Q. Li, "A new multi-objective discrete robust optimization algorithm for engineering design," *Applied Mathematical Modelling*, vol. 53, pp. 602–621, 2018.

[26] F. Sanchez, M. Budinger, and I. Hazyuk, "Dimensional analysis and surrogate models for the thermal modeling of multiphysics systems," *Applied Thermal Engineering*, vol. 110, pp. 758–771, 2017.

[27] N. Taran, D. M. Ionel, and D. G. Dorrell, "Two-level surrogate-assisted differential evolution multi-objective optimization of electric machines Using 3-D FEA," *IEEE Transactions on Magnetics*, vol. 54, no. 11, pp. 1–5, 2018.

[28] F. Li, G. Sun, X. Huang, J. Rong, and Q. Li, "Multiobjective robust optimization for crashworthiness design of foam filled thin-walled structures with random and interval uncertainties," *Engineering Structures*, vol. 88, pp. 111–124, 2015.

[29] F. Li, J. Liu, G. Wen, and J. Rong, "Extending SORA method for reliability-based design optimization using probability and convex set mixed models," *Structural and Multidisciplinary Optimization*, pp. 1–17, 2018.

[30] J.-M. Bourinet, "Rare-event probability estimation with adaptive support vector regression surrogates," *Reliability Engineering & System Safety*, vol. 150, pp. 210–221, 2016.

[31] Z. Wang and M. Ierapetritou, "A novel feasibility analysis method for black-box processes using a radial basis function adaptive sampling approach," *AIChE Journal*, vol. 63, no. 2, pp. 532–550, 2017.

[32] N. Le Chau, M.-Q. Nguyen, T.-P. Dao, S.-C. Huang, T.-C. Hsiao, D. Dinh-Cong et al., "An effective approach of adaptive neuro-fuzzy inference system-integrated teaching learning-based optimization for use in machining optimization of S45C CNC turning," *Optimization and Engineering*, pp. 1–22, 2018.

[33] S.-C. Kang, H.-M. Koh, and J. F. Choo, "An efficient response surface method using moving least squares approximation for structural reliability analysis," *Probabilistic Engineering Mechanics*, vol. 25, no. 4, pp. 365–371, 2010.

[34] M. A. Bezerra, R. E. Santelli, E. P. Oliveira, L. S. Villar, and L. A. Escaleira, "Response surface methodology (RSM) as a tool for optimization in analytical chemistry," *Talanta*, vol. 76, no. 5, pp. 965–977, 2008.

[35] D. Baş and I. H. Boyaci, "Modeling and optimization I: usability of response surface methodology," *Journal of Food Engineering*, vol. 78, no. 3, pp. 836–845, 2007.

[36] M.-R. Kolahi, A. Nemati, and M. Yari, "Performance optimization and improvement of a flash-binary geothermal power plant using zeotropic mixtures with PSO algorithm," *Geothermics*, vol. 74, pp. 45–56, 2018.

[37] M. Soruri, J. Sadri, and S. H. Zahiri, "Gene clustering with hidden Markov model optimized by PSO algorithm," *Pattern Analysis and Applications*, vol. 21, no. 4, pp. 1121–1126, 2018.

[38] O. Aoun, M. Sarhani, and A. El Afia, "Hidden markov model classifier for the adaptive particle swarm optimization," in *Recent Developments in Metaheuristics*, vol. 62, pp. 1–15, Springer, 2018.

[39] Y. Zhang, S. Wang, and G. Ji, "A comprehensive survey on particle swarm optimization algorithm and its applications," *Mathematical Problems in Engineering*, vol. 2015, Article ID 931256, 38 pages, 2015.

[40] X. Hu and R. Eberhart, "Solving constrained nonlinear optimization problems with particle swarm optimization," in *Proceedings of the Sixth World Multiconference on Systemics, Cybernetics and Informatics*, pp. 203–206, 2002.

[41] N. Ben Guedria, "Improved accelerated PSO algorithm for mechanical engineering optimization problems," *Applied Soft Computing*, vol. 40, pp. 455–467, 2016.

[42] N. L. Ho, T. Dao, N. Le Chau, and S. Huang, "Multi-objective optimization design of a compliant microgripper based on hybrid teaching learning-based optimization algorithm," *Microsystem Technologies*, pp. 1–17, 2018.

[43] S.-C. Huang and T.-P. Dao, "Multi-objective optimal design of a 2-DOF flexure-based mechanism using hybrid approach of Grey-Taguchi coupled response surface methodology and entropy measurement," *Arabian Journal for Science and Engineering*, vol. 41, no. 12, pp. 5215–5231, 2016.

[44] G. Zheng, S. Wu, G. Sun, G. Li, and Q. Li, "Crushing analysis of foam-filled single and bitubal polygonal thin-walled tubes," *International Journal of Mechanical Sciences*, vol. 87, pp. 226–240, 2014.

[45] F. Orlhac, C. Nioche, M. Soussan, and I. Buvat, "Understanding changes in tumor texture indices in PET: a comparison between visual assessment and index values in simulated and patient data," *Journal of Nuclear Medicine*, vol. 58, no. 3, pp. 387–392, 2017.

[46] T.-P. Dao and S.-C. Huang, "Design, fabrication, and predictive model of a 1-dof translational flexible bearing for high precision mechanism," *Transactions of the Canadian Society for Mechanical Engineering*, vol. 39, no. 3, pp. 419–429, 2015.

[47] S. Nikbakt, S. Kamarian, and M. Shakeri, "A review on optimization of composite structures Part I: laminated composites," *Composite Structures*, vol. 195, pp. 158–185, 2018.

[48] M. Mehdinejad, B. Mohammadi-Ivatloo, and R. Dadashzadeh-Bonab, "Energy production cost minimization in a combined heat and power generation systems using cuckoo optimization algorithm," *Energy Efficiency*, vol. 10, no. 1, pp. 81–96, 2017.

[49] Z. Cui, B. Sun, G. Wang, Y. Xue, and J. Chen, "A novel oriented cuckoo search algorithm to improve DV-Hop performance for cyber–physical systems," *Journal of Parallel and Distributed Computing*, vol. 103, pp. 42–52, 2017.

[50] T.-P. Dao, S.-C. Huang, and P. T. Thang, "Hybrid Taguchi-cuckoo search algorithm for optimization of a compliant focus positioning platform," *Applied Soft Computing*, vol. 57, pp. 526–538, 2017.

[51] M. Yasar, "Optimization of reservoir operation using cuckoo search algorithm: example of adiguzel dam, Denizli, Turkey," *Mathematical Problems in Engineering*, vol. 2016, Article ID 1316038, 7 pages, 2016.

[52] H. J. Shin, M.-J. Kim, H. Y. Kim, Y. H. Roh, and M.-J. Lee, "Comparison of shear wave velocities on ultrasound elastography between different machines, transducers, and acquisition depths: a phantom study," *European Radiology*, vol. 26, no. 10, pp. 3361–3367, 2016.

[53] N. Veček, M. Črepinšek, and M. Mernik, "On the influence of the number of algorithms, problems, and independent runs in the comparison of evolutionary algorithms," *Applied Soft Computing*, vol. 54, pp. 23–45, 2017.

[54] M. Mückschel, K. Gohil, T. Ziemssen, and C. Beste, "The norepinephrine system and its relevance for multi-component behavior," *NeuroImage*, vol. 146, pp. 1062–1070, 2017.